Supporting Information

Introducing an alternative oxidant for Spiro-OMeTAD with the reduction product to passivate perovskite defects

Xing Gao[a], Fei Wu[a,*],Ye Zeng[a], Kaixing Chen[a], Xiaorui Liu[b,*], Linna Zhu[a,*]

[a] *Chongqing Key Laboratory for Advanced Materials and Technologies of Clean Energy, School of Materials & Energy, Southwest University, Chongqing 400715, P. R. China.*

[b] *Key Laboratory of Luminescence Analysis and Molecular Sensing, Ministry of Education, School of Chemistry and Chemical Engineering, Southwest University, Chongqing 400715, P. R. China.*

Corresponding Author: *Linna Zhu, School of Materials & Energy, Southwest University, Chongqing, China, E-mail address: lnzhu@swu.edu.cn.*

Fei Wu, School of Materials & Energy, Southwest University, Chongqing, China, E-mail address: feiwu610@swu.edu.cn.

Xiaorui Liu, School of Chemistry and Chemical Engineering, Southwest University, Chongqing, China, E-mail address: liuxiaorui@swu.edu.cn.

Table of Contents

1. Experimental Section

2. Calculation formulas

3. Figures:

Figure S1. Photograph of different spiro-OMeTAD solutions undergoing thin-film chromotography.

Figure S2. ^{1}H NMR spectrum of the reduction product of IBX.

Figure S3. XPS spectra of the I 3d of the perovskite film and perovskite/2-Iodobenzoic acid film.

Figure S4. XPS spectra of the I 3d of the 2-Iodobenzoic acid film.

Figure S5. XPS spectra of the C 1s of different films.

Figure S6. SEM images of spiro-OMeTAD films without (a) and with IBX (b).

Figure S7. *J-V* curve of hole-only devices based on unoxidized Spiro-OMeTAD.

Figure S8. TRPL spectra of perovskite substrate with different HTL films.

Figure S9. $J-V$ curves of the devices based on spiro-OMeTAD with different concentrations of IBX.

Figure S10. Statistical distribution of photovoltaic parameters of the PSCs doped with or without IBX: J_{sc} (a), V_{oc} (b), FF (c) and PCE (d).

Figure S11. TPV of the PSCs with and without IBX.

4. Tables:

Table S1. Conductivity of spiro-OMeTAD films with different treatments.

Table S2. Specific values of series resistance (R_s), and recombination resistance (R_{rec}) of PSCs with and without IBX.

Table S3. Photovoltaic parameters of the devices with different concentrations of IBX.

Table S4. Photovoltaic data of the PSCs based on spiro-OMeTAD with and without IBX scanned from different directions.

Experimental Section

Materials

Spiro-OMeTAD, Li-TFSI, tBP, Cesium iodide (CsI, 99.90%), Formamidinium iodide (FAI, 99.90%), Lead iodide (PbI_2, 99.99%) and Lead bromide ($PbBr_2$, 99.99%) were purchased from Youxuan Tech.. N,N-Dimethylformamide (DMF, 99.80%), Dimethyl sulfoxide (DMSO, 99.80%), Chlorobenzene (CB, 99.80%) and Acetonitrile (ACN) were purchased from Sigma-aldrich. 30 NR-D transparent Titania paste was purchased from Xi'an Polymer Light Technology Corp. 2-Iodoxybenzoic acid (IBX, 97.00%) was purchased from Energy Chemical.

Solution preparation

The perovskite precursor solution was prepared by dissolving 1.30 M PbI_2, 1.19 M FAI, 0.14 M $PbBr_2$, 0.14 M MABr, and 0.07 M CsI into the DMSO/DMF (1/4, v/v) mixture. The hole transport material solution was prepared by dissolving 72.5 mg of spiro-OMeTAD in 1mL of CB, with the additives of 28.5 μL t-BP, 17.5 μL Li-TFSI (520 mg mL^{-1} in ACN). For the spiro-OMeTAD solution with IBX, IBX was added into HTL precursor solution, the concentration of IBX were 1.0 mg mL^{-1}, 1.5 mg mL^{-1}, 2.0 mg mL^{-1}, 2.5 mg mL^{-1}, and 3.0 mg mL^{-1}, respectively.

Fabrication of perovskite solar cells

The FTO glass substrates (14 Ω per square) were ultrasonically cleaned with detergent, deionized water and ethanol for 20 min in sequence, and dried by nitrogen flow. Then the dry FTO substrates were treated by O_2-plasma for 180 s before using.

After that, a compact TiO_2 layer was deposited on the cleaned FTO glass by spray pyrolysis from a precursor solution of 0.2 M titanium isopropoxide and 2 M acetylacetone in isopropanol. The mesoporous TiO_2 was prepared by diluting a commercial TiO_2 paste (30 NR-D) with anhydrous ethanol at a weight ratio of 1/6. After sintering the compact TiO_2, the mesoporous TiO_2 layer was spin-coated onto the TiO_2 compact layer at 5000 rpm for 30 s, and sintered. The perovskite film was deposited by a consecutive two-step spin-coating process at 2000 rpm for 10 s and then at a speed of 6000 rpm for 30 s on the surface of mesoporous TiO_2 layer. At the time of 15 s prior to the program end, 100 μL of chlorobenzene was dripped on the spinning substrate, and then the film was annealed at 120 ℃ for 1 h. The spiro-OMeTAD solution (with or without IBX) was spin-coated on the perovskite film at 6000 rpm for 30 s. Finally, 60 nm thick Au film was thermally evaporated on the HTL in vacuum environment ($<10^{-5}$Pa) to accomplish the whole fabrication of device.

Characterizations

UV-vis absorption spectra were measured on a Shimadzu UV-2550 absorption spectrophotometer. Fluorescence emission spectra was measured by fluorescence spectrophotometer (RF-5301PC). The space-charge limited current (SCLC) measurements were performed by collecting the *J–V* characteristics of devices in dark conditions. The Fourier-transform infrared spectroscopy (FTIR) spectroscopy was carried out using Thermo Nicolet 6700. The current-voltage (*J-V*) characteristics were measured under 100 mW cm^{-2} (AM 1.5G illumination) using a Newport solar simulator (model 91160) and a Keithley 2400 source/meter. PL and TR-PL spectra

were obtained via using the Pico Quant Fluotime 300 with a 510 nm picosecond pulsed laser. The surface morphology of films was characterized by FE-SEM images (JSM-7800F), and atomic force microscope (AFM) was used for characterizing the morphology using a CSPM5500. X-ray photoelectron spectroscopy (XPS) was performed using a scanning XPS microprobe (K-Alpha). The EIS were measured with CHI 6500 in the dark. Film thickness were measured with Surfcorder ET150. Transient photocurrent (TPC) and transient photovoltage (TPV) were recorded using a ZAHNE®MESSSYSTEME (Instrument model: PP211).

Hole Mobility Measurements

Devices structure: FTO/PEDOT:PSS/Spiro-OMeTAD with or without IBX/MoO_3/Ag

The hole mobilities (μ) were measured by using space charge limited current (SCLC) method with an equation as follows:

$$J = \frac{9\varepsilon_0\varepsilon_r\mu V^2}{8L^3}$$

where ε_0 and ε_r are the vacuum permittivity (8.85×10^{-12} F/m) and relative permittivity, respectively. J is the current density, μ is the hole mobility, V is voltage, and L is the film thickness.

Conductivity Measurements

Devices structure：FTO/Spiro-OMeTAD with or without IBX/Ag

The conductivity of spiro-OMeTAD films with or without IBX is characterized by J–V curves. The conductivity was calculated according to the following equation:

$$\sigma = Id/AV$$

where A is the active area of the device, d is the thickness of the films, I is the current, and V is the voltage.

TRPL Analysis

The TRPL results are fitted through the biexponential equation as below:

$$f(t) = A_1 \exp\left(\frac{-t}{\tau_1}\right) + A_2 \exp\left(\frac{-t}{\tau_2}\right)$$

And the average value of lifetime ($\tau_{ave.}$) is calculated by the following equation:

$$\tau_{ave.} = \frac{A_1 * \tau_1^2 + A_2 * \tau_2^2}{A_1 * \tau_1 + A_2 * \tau_2}$$

τ_1 and τ_2 represent the fast and slow decay times, which are derived from the charge carriers quenching and the radiative recombination, respectively.

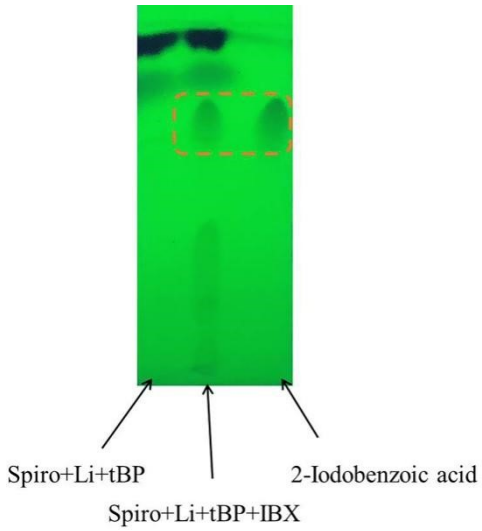

Figure S1. Photograph of different spiro-OMeTAD solutions undergoing thin-film chromotography.

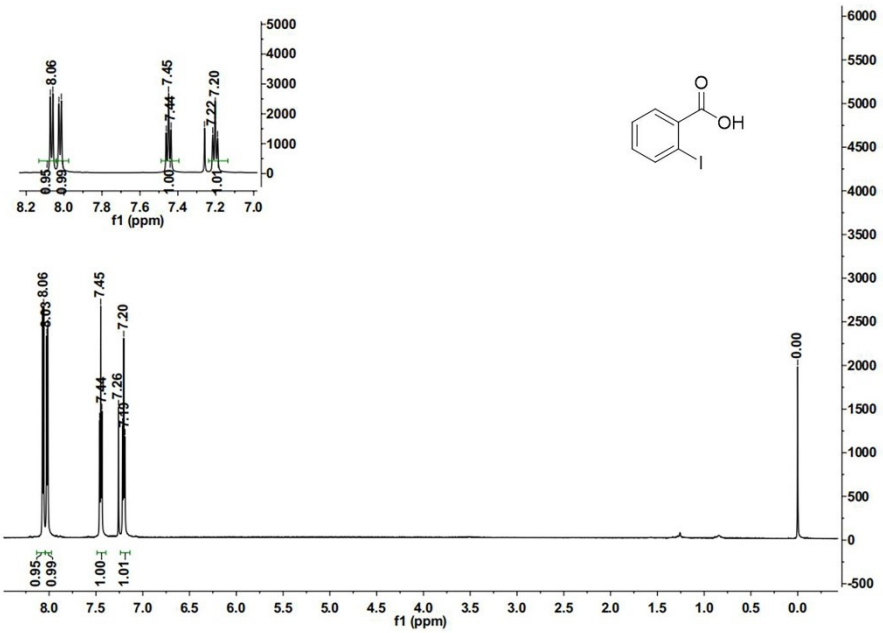

Figure S2. ^{1}H NMR spectrum of the reduction product of IBX.

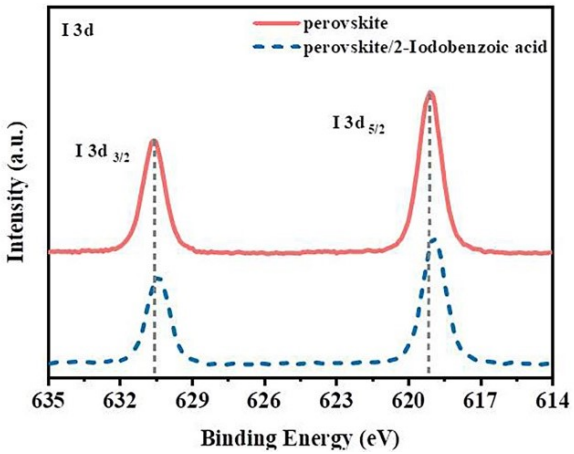

Figure S3. XPS spectra of the I 3d of the perovskite film and perovskite/2-Iodobenzoic acid film.

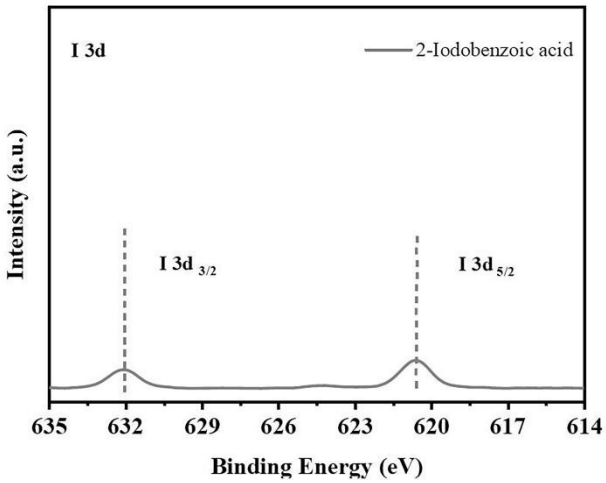

Figure S4. XPS spectra of the I 3d of the 2-Iodobenzoic acid film.

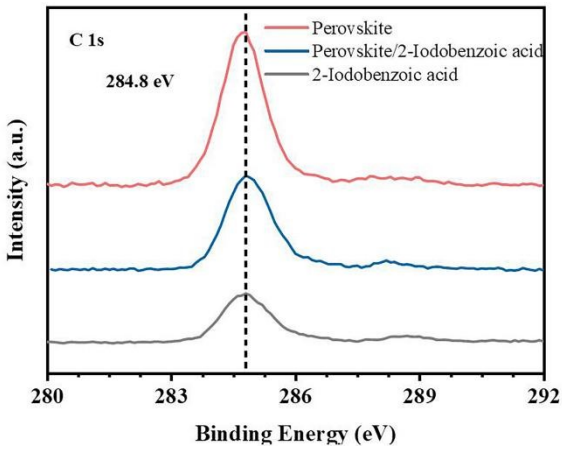

Figure S5. XPS spectra of the C 1s of different films.

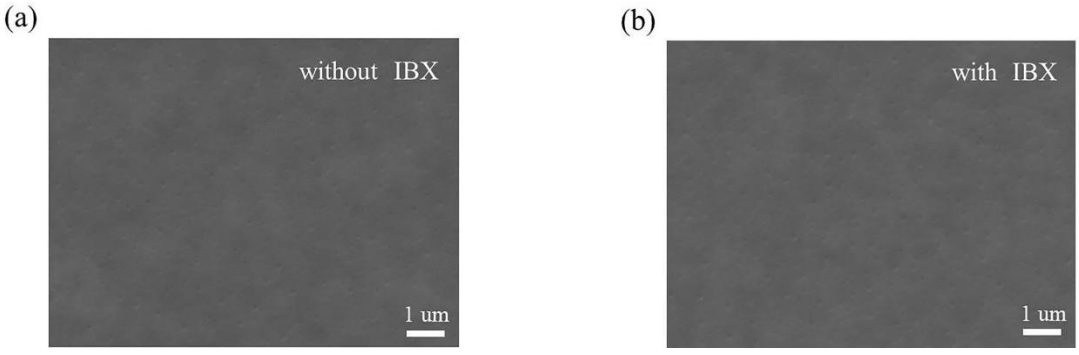

Figure S6. SEM images of spiro-OMeTAD films without (a) and with IBX (b).

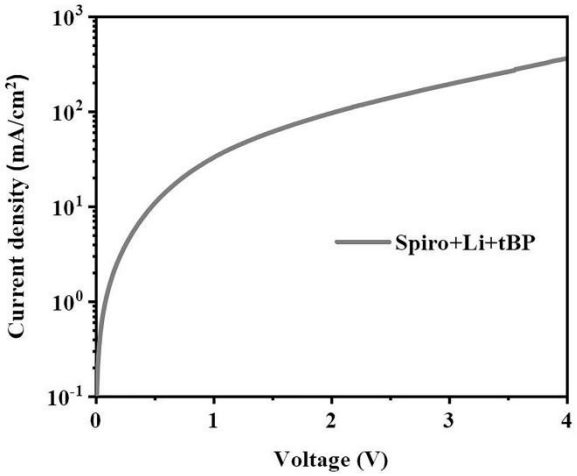

Figure S7. J-V curve of hole-only devices based on unoxidized Spiro-OMeTAD.

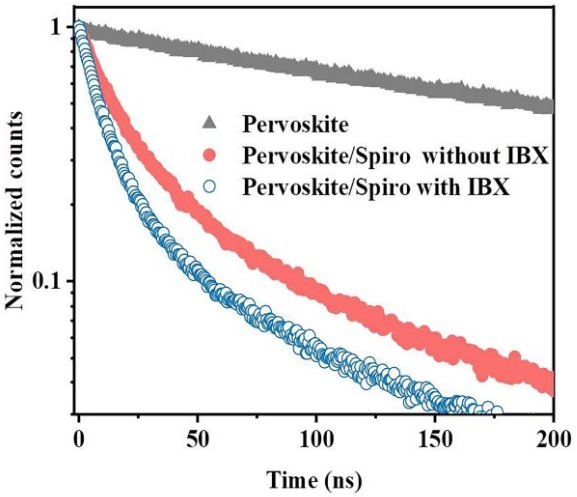

Figure S8. TRPL spectra of perovskite substrate with different HTL films.

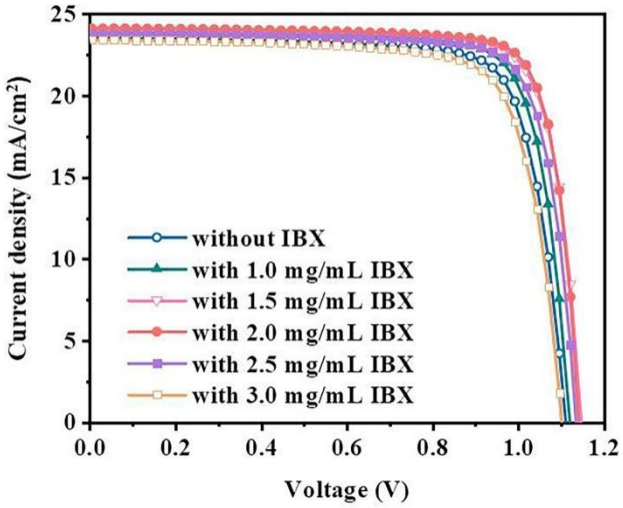

Figure S9. $J-V$ curves of the devices based on spiro-OMeTAD with different concentrations of IBX.

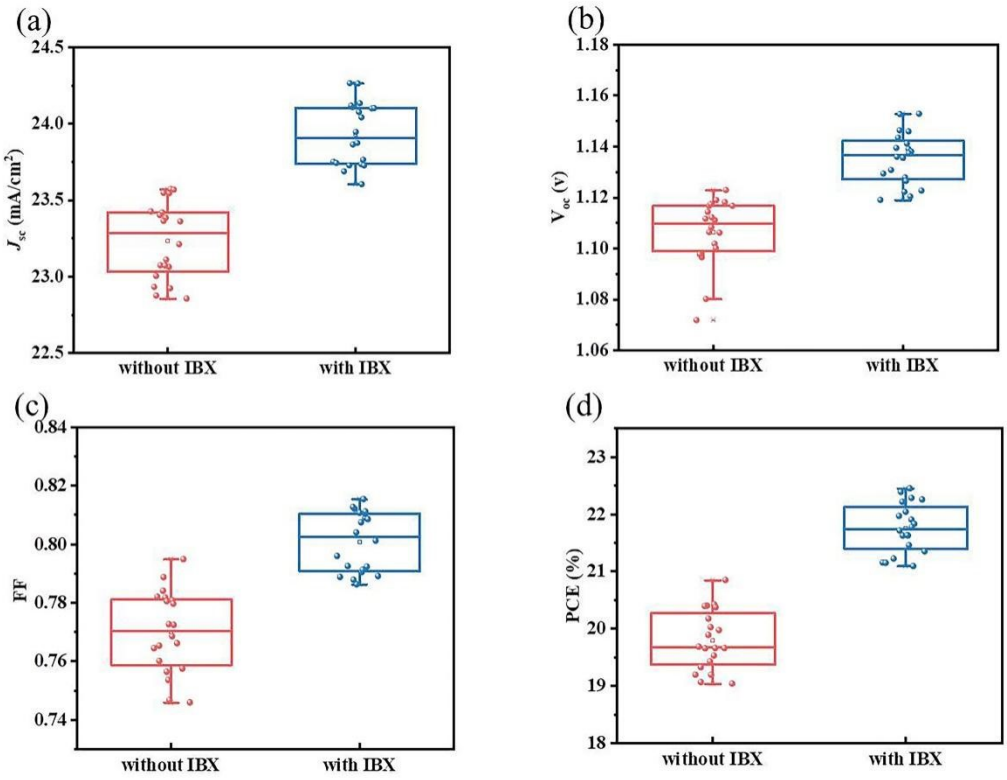

Figure S10. Statistical distribution of photovoltaic parameters of the PSCs doped with or without IBX: J_{sc} (a), V_{oc} (b), FF (c) and PCE (d).

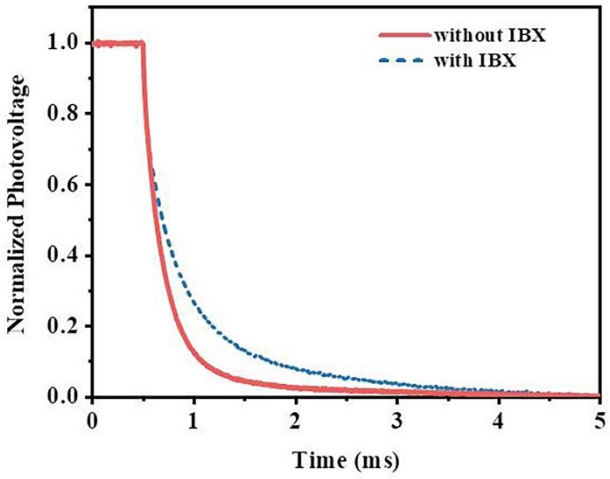

Figure S11. TPV of the PSCs with and without IBX.

Table S1. Conductivity of spiro-OMeTAD films with different treatments.

Sample	$S \cdot cm^{-1}$
spiro+Li+tBP	3.8×10^{-5}
spiro+Li+tBP+O_2	8.7×10^{-5}
spiro+Li+tBP+IBX	1.5×10^{-4}

Table S2. Specific values of series resistance (R_s), and recombination resistance (R_{rec}) of PSCs with and without IBX.

Devices	R_s (Ω)	R_{rce} (Ω)
without IBX	23	2135
with IBX	20	4180

Table S3. Photovoltaic parameters of the devices with different concentrations of IBX.

Doping concentration （mg/mL）	J_{sc} (mA/cm^2)	V_{oc} (V)	FF	PCE (%)
0.0	23.54	1.11	0.78	20.42
1.0	23.88	1.12	0.79	21.25
1.5	24.01	1.14	0.81	22.22
2.0	24.13	1.14	0.82	22.45
2.5	23.80	1.13	0.80	21.55
3.0	23.42	1.10	0.76	19.70

Table S4. Photovoltaic data of the PSCs based on spiro-OMeTAD with and without IBX scanned from different directions.

Doping	Scan direction	J_{sc} (mA/cm^2)	V_{oc} (V)	FF	PCE (%)
Without IBX	Forward	23.54	1.11	0.78	20.42
	Reverse	23.49	1.10	0.75	19.29
With IBX	Forward	24.13	1.14	0.82	22.45
	Reverse	24.11	1.13	0.79	21.66